The effects of film thickness and incorporated anions on pitting corrosion of aluminum with barrier-type oxide films formed in neutral borate and phosphate electrolytes

Hiroki Habazaki[1,*], Rokuro Nishimura[2,*], Kenji Okitsu[2], Hiroyuki Inoue[2], Ikuo Kiriyama[2], Fumitaka Kataoka[3], Masatoshi Sakairi[4] and Hideaki Takahashi[5]

[1]Division of Materials Chemistry & Frontier Chemistry Center, Faculty of Engineering, Hokkaido University, Sapporo, Hokkaido 060-8628, Japan

[2]Graduate School of Engineering, Osaka Prefecture University, 1-1, Gakuen-cho, Sakai, Osaka 599-8531, Japan.

[3]Graduate School of Chemical Sciences and Engineering, Hokkaido University, Sapporo, Hokkaido 060-8628, Japan

[4]Division of Materials Science and Engineering, Faculty of Engineering, Hokkaido University, Sapporo, Hokkaido 060-8628, Japan

[5]Asahikawa National College of Technology, Syunkohdai, 2-2, 1-6, Asahikawa 071-8142, Japan

Corresponding author.

e-mail address: nishimu@mtr.osakafu-u.ac.jp (R. Nishimura) and habazaki@eng.hokudai.ac.jp (H. Habazaki).

Abstract

The pitting corrosion behavior of high purity aluminum covered with barrier-type anodic films, which are formed in neutral borate and phosphate electrolytes, has been examined in 0.5 mol dm^{-3} NaCl solution at an applied potential of -0.6 V vs Ag/AgCl, which is slightly nobler than the pitting potential of -0.64 V in the same solution. The pitting current density, i_p, increased with time after an incubation time, t_i. The double logarithmic plot of i_p and polarization time, t, reveals two straight lines, which are separated at the time, τ. The slope becomes larger after τ for the specimens anodized in the phosphate electrolyte, while it becomes smaller for those in the borate electrolyte. Both the t_i and τ increase with the thickness of the anodic films, and at the similar film thickness they are much larger for the anodic films formed in the phosphate electrolyte than for those in the borate electrolyte. The corrosion process can be divided into three stages; the incubation period up to t_i, the pit nucleation period before τ and the pit growth period after τ. We have discussed the different pitting corrosion behavior of the aluminum specimens covered with the anodic films formed in the borate and phosphate electrolytes in terms of ion selectivity of the anodic films.

Keywords: Aluminum, pitting corrosion, anodic film, chloride solution, ion selectivity.

1. Introduction

Pitting corrosion of aluminum and its alloys has been widely investigated and excellently reviewed by Foley [1] and Smialowska [2]. The pitting process is generally divided into the following four steps [1]; (1) the adsorption of the reactive anions, such as chloride, on the oxide-covered aluminum, (2) the chemical reaction of the adsorbed anions with the aluminum oxide, (3) the thinning of the oxide film by dissolution and (4) the direct attack of the exposed metal by the anions, in which the steps (1) to (3) correspond to a nucleation period and the step (4) to a growth period. In addition, in accord with Smialowska [2], the first two steps are dependent upon the composition and structure of the oxide film, including the material composition, the presence and distribution of micro-defects, such as vacancies and voids, macro-defects, such as inclusions and second phase particles and so on. Recent studies on pitting corrosion of aluminum and its alloys have been carried out under the consideration of the pitting process described above [3-6]. The role of various additive anion species on pitting corrosion of aluminum has also been examined [7-9].

On the other hand, ion selectivity of the surface oxide films on metals and alloys is of crucial importance on their corrosion. The protective properties of the rust layers formed on various steels have often been discussed in terms of the ion selectivity of the rust layers [10-15]. The pitting corrosion of metals covered with a thin passive film has also been discussed in terms of the ion selectivity. Nishimura et al. investigated pitting corrosion of high purity iron [16] and nickel [17], covered with a thin passive film, at a potential nobler than a critical pitting potential in 0.5 mol dm^{-3} NaCl solution. The passive films were formed as a function of applied potential in borate and phosphate solutions with various pHs. The results obtained indicated that their pitting corrosion behavior was largely influenced by ion selectivity (anion or cation selectivity) of the

passive films. The metals covered with the passive films formed in the neutral borate solution, having the anion selective property, had much less pitting corrosion resistance than those formed in the neutral phosphate solution, which had the cation selective property. When the passive films were formed in the alkaline borate solution, iron showed the increase in the pitting corrosion resistance in comparison with that formed in the neutral borate solution because of the change in ion selectivity from anion selectivity to cation one. In contrast, iron covered with the passive film formed in the alkaline phosphate solution showed the decrease in the pitting corrosion resistance, compared to that formed in the neutral phosphate solution, because of the reduction of cation selectivity. The pitting corrosion behavior of nickel covered with passive films formed in the borate and phosphate electrolytes showed little dependence of anion species and pH, being different from the pitting behavior of iron. This was considered that the ion selectivity of the passive films, showing anion selectivity, had little change with pH and anion species. Thus, it was concluded that the ion selectivity of the thin passive films played an important role in their pitting corrosion behavior.

Aluminum can form a relatively thick, barrier-type anodic oxide film in neutral aqueous electrolytes. However, to our knowledge, there is no investigation on the influence of the ion selectivity of the aluminum oxide films on the pitting corrosion behavior of aluminum. The anodic oxide films formed on aluminum are generally contaminated with electrolyte anion species and their distribution and contents have been characterized [18]. In addition, the thickness of the anodic oxide films can be controlled readily by the anodizing potential. Thus, in the present study, we tried to elucidate a relationship between ion selectivity of the anodic film and pitting corrosion behavior of aluminum, referring to the results of iron and nickel [16,17]. The barrier-type anodic films have been formed on aluminum at several anodizing potentials in borate-buffer and phosphate-buffer electrolytes. Pitting corrosion behavior has been

examined in 0.5 mol dm^{-3} NaCl solution at the potential slightly nobler than the pitting potential of -0.64 V vs Ag/AgCl.

2. Experimental

High purity (99.99%) aluminum sheet of 2 mm thickness was used in this study. Prior to the experiments, the specimens were polished with an emery paper of 2000 grit and electropolished at a current density of 0.12 A cm^{-2} for 3 min in a 1:4 mixture of 60% perchloric acid and glacial acetic acid at 288 K, followed by washing in distilled water. After electropolishing, the specimens were immersed in a mixed solution of 0.2 mol dm^{-3} H_3PO_4 and 0.54 mol dm^{-3} H_2CrO_4 for 10 min at 353 K to remove a formed electropolishing film containing chloride species [19]. The specimens thus pretreated were covered with an Araldite resin to expose about 1.0 cm^2 of specimen surface. Then, anodizing was carried out by applying a constant current density of i_a = 1 mA cm^{-2} until the anodic potential reached a selected potential in a range of 5 to 100 V vs Ag/AgCl. The electrolytes used for anodizing were a borate solution of 0.5 mol dm^{-3} H_3BO_4-0.05 mol dm^{-3} $Na_2B_4O_7$ with pH = 7.4 and a phosphate solution of 0.033 mol dm^{-3} $NH_4H_2PO_4$- 0.067 mol dm^{-3} $(NH_4)_2HPO_4$ with pH = 7.0. In these neutral electrolytes the anodic films formed are barrier-type, not porous-type [20,21]. The solution for pitting corrosion studies of the anodized specimens was 0.5 mol dm^{-3} NaCl solution, which was deaerated with argon gas before and during experiments. The test temperature was 293 K for all experiments.

After anodizing to 100 V vs Ag/AgCl, the specimens were observed by a JEOL JEM2000FX transmission electron microscope operating at 200 kV. Electron transparent sections were prepared using ultramicrotomy. Elemental depth profile analysis of the anodic films was carried out by glow discharge optical emission spectroscopy (GDOES) using a Jobin-Yvon 5000 RF instrument in an argon atmosphere

of 850 Pa by applying RF of 13.56 MHz and power of 35W. Light emissions of characteristic wavelengths were monitored throughout the analysis with a sampling time of 0.01s to obtain depth profiles.

In order to determine the polarization potential for pitting corrosion studies, a critical pitting potential of the high purity aluminum without anodizing was measured in 0.5 mol dm^{-3} NaCl solution at 293 K by a potential step method (0.05 V step for 600 s interval) [16,17]. The critical pitting potential determined was -0.64 V vs Ag/AgCl, which was an average value with an accuracy of ±0.01 V through several trials. For the aluminum covered with anodic films, a constant potential of -0.6 V vs Ag/AgCl, which was slightly nobler than the critical pitting potential, was applied. Then, the current transient during the polarization was measured for all anodized specimens.

3. Results

3.1 Characterization of the anodic films

Fig. 1 shows transmission electron micrographs of ultramicrotomed sections of aluminum anodized to 100 V vs Ag/AgCl in the borate (Fig. 1(a)) and phosphate (Fig. 1(b)) electrolytes. An anodic film with flat and parallel metal/film and film/electrolyte interface is developed on aluminum substrate, which appears at the bottom of the micrographs. The anodic films are relatively featureless and no diffraction contrast is seen in the anodic films, indicating that the anodic films are amorphous. The thickness of the anodic films is 130 ± 2 nm regardless of the electrolyte used. Thus, the formation ratio of the anodic films is 1.3 nm V^{-1}. Using this value, the thicknesses of the anodic films formed at various formation potentials can be estimated.

The depth distribution of the electrolyte-derived species, i.e., boron and phosphorus species, was examined by the GDOES elemental depth profile analysis. Obviously, both boron and phosphorus species are incorporated into the anodic films

and distributed in the outer part of the anodic films (Fig. 2). However, their distribution depth is dependent upon the species. The boron species are present in the outer ~40% of the film thickness, while the phosphorus species distribute to the depth of ~75% of the film thickness. The different distribution of boron and phosphorus species is owing to the mobility of the electrolyte-derived species, as discussed below.

Previously, the average compositions of the anodic films formed in various electrolytes at a constant current density of 50 A m^{-2} at 293 K were estimated from the total numbers of Al, O and X (X=B and P) in the anodic films [18]. The average film compositions formed in the borate and phosphate are $Al_2O_{3.07}{\cdot}P_{0.06}$, $Al_2O_{3.17}{\cdot}P_{0.072}$, respectively, indicating that similar amounts of boron and phosphorus species are incorporated into the anodic alumina films.

3.2 Time variation of pitting current density

3.1.1 Anodic films formed in borate electrolyte

Fig. 3 shows the pitting current density, i_p, and time, t, curves for aluminum covered with anodic films of various thicknesses, formed in the borate solution. The result of the specimen without anodic film is also shown as a dashed line for comparison. Obviously, i_p decreases with an increase in film thickness, although i_p increases with time for all specimens. In these curves, the presence of an incubation time, t_i, below which i_p is negligibly small, is not obvious and the i_p - t curves for the specimens with anodic films appear to consist of two straight lines with a different slope. To make them clearer, the logarithmic relationships of the i_p - t curves are drawn in Fig. 4. All the curves for the specimens with the anodic films of three different thicknesses show two different straight lines, in which the inflection between two straight lines occurs at the time, τ. The slope of the first straight line became larger than that of the second straight line.

3.1.2 Anodic films formed in phosphate electrolyte

Fig. 5 shows the i_p - t curves for aluminum covered with anodic films of various thicknesses, formed in the phosphate electrolyte. Again, i_p decreases with an increase in the thickness over the whole time range. Compared to those in Fig. 3, it took a longer time for i_p to increase and t_i was detected clearly for the anodic films with the thicknesses of 98 and 130 nm. The logarithmic relationships of the i_p- t curves, shown in Fig. 6, show clearly the two different straight lines, except the thickness of 130 nm, as the films formed in the borate electrolyte (Fig. 4). For the anodic films formed in the phosphate electrolyte, however, the slope of the first straight line is smaller than that of the second straight line, which is the opposite to that in Fig. 4. The log i_p - log t curve for the anodic film of 130 nm thickness shows complex behavior, so that it may be difficult or uncertain to determine τ. However, by simply assuming the two straight lines with the similar slopes as those in the other curves, the τ value is estimated from the dashed lines in Fig. 6.

3.2. Effects of thickness and anion species on incubation time (t_i)

In this study, we determined approximately t_i from Figs. 4 and 6 as follows. When the first straight lines are extrapolated to the time axis at 1 x 10^{-6} A cm^{-2} on the vertical axis in Figs. 4 and 6, the time at the intersection point is assumed to be t_i. Fig. 7 shows the relationship between t_i with a logarithmic scale and thickness (L) of the anodic films formed in the borate and phosphate electrolytes. In both the anodic films, log t_i increases linearly with the film thickness. At each film thickness, t_i in the phosphate electrolyte is always larger than that in the borate electrolyte.

3.3 Effect of thickness and anion species on τ

Fig. 8 shows the relationships between τ and L of the anodic films formed in the borate and phosphate electrolytes. For the anodic films formed in the borate electrolyte, a good linear correlation is obtained between τ and L. Similarly, a linear correlation is found for the anodic films formed in the phosphate electrolyte until the film thickness is 100 nm. The τ for the anodic film of 130 nm thickness, which is roughly estimated from the dashed line in Fig. 6 is ~15 ks. The value estimated is considerably larger than that estimated from the extrapolation of the linear relationship up to 100 nm thickness (5.4 ks). The τ value in the phosphate electrolyte is larger than that in the borate electrolyte by a factor of 10～15.

4. Discussion

4.1 Ion-selective property of anodic films

Barrier-type anodic films formed on aluminum consist of two layers, comprising an outer layer contaminated with electrolyte anion-derived species and an inner layer of relatively pure Al_2O_3 [18,19,21]. The depth distribution of the electrolyte anion-derived species is controlled by the transport numbers of anion and cation and the mobility of the electrolyte anion-derived species [18]. The anodic films formed on aluminum are usually amorphous and developed both at the metal/film and film/electrolyte interfaces [22]. The transport number of cations of the anodic films on aluminum, determined by various marker studies, is ~0.4 [23-26], such that the outer 40% of the film material is formed at the film/electrolyte interface. The boron species incorporated from the borate electrolyte are immobile in the growing anodic films at high current efficiency, distributing in the outer 40% of the film thickness (Fig. 2(a)). Thus, the boron species should be present as neutral species, such as B_2O_3, in the growing anodic film. In contrast, phosphorus species are mobile inwards, distributing in the outer 75% of the film thickness, as shown in Fig. 2(b). The inward migration of the phosphorus species

incorporated from the phosphate electrolyte suggests the presence of anion species, such as PO_4^{3-}, in the growing anodic films under the high electric field.

It has been reported that the passive films on iron consists of two layers [27-29]. The outer layer is composed of hydroxide and the inner layer is oxide; the former layer includes electrolyte anion species. Therefore, the important point is that the barrier-type anodic films have the layer structure similar to that of the iron passive films, although the former anodic films are markedly thicker than the passive films on iron. For example the thickness of iron passive film is less than about 7 nm, while that of anodic films is as thick as 130 nm at maximum. Here, both thicknesses of the outer layer and the inner layer for the barrier-type oxide film increase proportionally with increasing anodizing potential with the thickness ratio being constant.

In the previous paper [16], the pitting corrosion behavior of iron covered with passive films formed in borate and phosphate solutions was examined as a function of solution pH and film thickness. The solution and applied potential used for pitting corrosion study were 0.5 mol dm^{-3} NaCl solution and -0.195 V vs SHE, respectively, the latter of which was nobler than the critical pitting potential. As in the present study, the pitting corrosion of iron with passive films formed in the phosphate solution at pH 8.42 has more pitting corrosion resistance than those formed in the borate solution at the same pH. The higher pitting corrosion resistance of iron covered with the passive films formed in the phosphate solution was explained in term of the ion selectivity of the outer layer of the passive film; the phosphate-containing films have cation-selectivity, while the borate-containing film is anion-selective. This suggests that the films with cation selectivity should have the higher resistance to the ingress (diffusion or migration) of chloride ions into the films than those with anion selectivity. The pitting corrosion behavior of nickel covered with thin passive films was also interpreted in terms of ion selectivity [17]. Although the passive films on iron and nickel are thin and

less than 7 nm, the outer layer of the passive films appears to serve as the ion selective membrane and the ingress of chloride ions is controlled through the pores in the outer layer, but not flaws or defects.

Provided that the anodic films formed on aluminum in the borate and phosphate electrolytes have the same ion selectivity as those on iron (anion selectivity or cation selectivity), we can explain the present results of high purity aluminum, showing the significant difference in t_i and τ, in terms of ion selectivity as described in the following sections. Fig. 9 shows a schematic representation of the ion selectivity of the anodic films formed in the borate and phosphate electrolytes. The anodic films with cation selectivity would make the ingress of chloride ions into the outer layer more difficult in comparison to those with cation selectivity, which is expressed as the difference of the length of arrows in the figure. Although, there is little data on the ion selective property of anodic films on aluminum, in contrast to that of the passive films on iron [16], it can be assumed that the boron species are electrically neutral because of their immobile nature during film growth, while the phosphorus species are anionic, such as PO_4^{3-}, due to their inward migration. The anionic phosphorus species-incorporated outer layer should have anion selectivity, suppressing the ingress of chloride anion. The precise mechanism of the ingress of chloride ions in the anodic alumina films is the subject of future study.

4.2 The meaning of t_i and τ

The time t_i is the time at which the pitting current density begins to increase with time, before which the pitting current density is negligibly small. As shown in Fig. 7, the t_i increases with an increase in film thickness and is significantly larger for the anodic films formed in the phosphate electrolyte than those in the borate electrolyte. It was assumed for iron that t_i would be defined as the time at which the inner layer begins

to be attacked to become thin or the destruction rate of the inner layer becomes larger than its formation rate (repassivation rate) [16]. In the present work, the anodic films were formed at high potentials. To increase the pitting current density, the ingress of chloride ion-containing solution into the anodic film to the depth below which a film of less than ~ 10 nm thickness is remained needs to occur. The ingress of chloride ions through the thick anodic films is slower for the films with cation selectivity in comparison with for the anion selectivity. Thus, the incubation time of t_i becomes longer in the anodic films formed in the phosphate electrolyte. The thicker anodic film also shows the longer incubation time.

After t_i, the relation between the pitting current density and time shows two different straight lines in the double logarithmic plot, as shown in Figs. 4 and 6, as for the passivated iron and nickel. It was pointed out for iron and nickel that the pitting current density before τ was the current density before the complete destruction of the inner layer and that after τ was the current density by the attack of substrate [16,17]. This would be applied to the current densities before and after τ, obtained in the present study. Therefore, τ is defined as the time up to the local complete destruction of the inner layer, and hence, it is reasonable to consider that τ increases with the increase in the thickness of the inner layer. On the other hand, the great difference in τ for anodic films in both solutions would be reasonable to be associated with the ion selectivity as well. The amount of chloride ions per time incorporated in the anodic films with cation selectivity would be less than that in the anodic films with anion selectivity, which was shown in Fig. 9 by a length of the arrow. Therefore, it would take a longer time for anodic films with cation selectivity than for anion selectivity to attack up to the local complete destruction of the inner layer.

After τ the direct attack of the exposed metal by the anion may occur. Therefore, we also call the period up to τ as the nucleation period and that after τ as the growth

period. In addition, τ may be called as the nucleation time. Thus, it is concluded that the pitting corrosion process of the anodized aluminum consists of the incubation, nucleation and growth periods.

4.3 Pitting current behavior before and after τ

The slope of the linear relationship between the pitting current density and time in the double logarithmic plot in the nucleation period, which is before τ, is close to 1.0 for both the anodic films formed in the borate and phosphate electrolytes (Figs. 4 and 6). This value was almost the same as that of passivated iron [16]. The slope of the linear relationship in the growth period, which is after τ, is dependent upon the electrolyte used. For the anodic films formed in the borate electrolyte, the slope in the growth period becomes smaller than that in the nucleation period, while the slope in the growth period becomes larger than that in the nucleation period for the anodic films formed in the phosphate electrolyte. For the passivated iron, however, the slope in the growth period is always larger than that in the nucleation period for both the passive films formed in the borate and phosphate electrolytes. It is generally considered that the pitting current density increases rapidly by the dissolution of the substrate (growth period), compared to that during the destruction of the inner layer (nucleation period), such that the slope after τ becomes larger than that before τ. Therefore, the pitting corrosion behavior after τ for the anodic films formed on aluminum in the borate solution appears to be unusual, but not for the anodic film in the phosphate solution.

The pitting corrosion during the growth period is usually considered to be diffusion or ohmic controlled [2]. However, under the same solution and polarization potential for pitting study, the difference in the slope in the growth period between the anodic films formed in both solutions cannot be explained by the diffusion- or ohmic-controlled process. Therefore, we need to consider another factor.

One of the most probable explanations is related to the formation of a salt film in the pits. It is well accepted that a salt film exists within aluminum pits and stabilizes the pits [2]. In chloride solutions, the salt film formed in the pits of aluminum is assumed to be composed of $AlCl_3$, $Al(OH)Cl_2$ and $Al(OH)_2Cl$ [30]. If the composition of the salt film is the same as that in the pits formed for aluminum covered with the anodic films formed in both electrolytes, it is likely that the growth rate of the pits would be the same, but not. Therefore, we estimate that the borate ions and phosphate ions are freely available in the pits by the dissolution of the outer layer and included in the salt film, forming $Al(OH)_n(X)_m$ (X = borate or phosphate). It can be assumed that the salt film with the borate ions has anion-selective property and that with the phosphate ions cation-selective property, similar to those of the outer layer. During the pit growth period the major reaction is the dissolution of Al^{3+} ions from the substrate. If the salt film has cation-selective property, it would be easy for aluminum ions to diffuse into the salt film and then to diffuse out into the electrolyte through salt film. On the other hand, it would be difficult to diffuse into the salt film with anion-selective property, so that an accumulation of Al^{3+} ions would occur at an interface between the substrate and salt film. This would serve as an inhibition for the dissolution of Al^{3+} ions. Thus, although the outer layer and the salt film are assumed to have the same ion-selective property, the effect of the ion selectivity on pitting corrosion depends upon the pitting corrosion process. Up to the nucleation period, the ingress of chloride ions into the outer layer makes an important role in pitting corrosion behavior and is affected by the ion-selective property, while at the growth period the diffusion (or migration) of Al^{3+} ions becomes important for the pitting corrosion behavior and is affected with the reverse trend compared to the pitting corrosion behavior up to the nucleation period.

5. Conclusions

(1) The pitting corrosion of pure aluminum with anodic films formed in the borate and phosphate solutions consists of the three periods of incubation, pit nucleation and pit growth.

(2) The incubation time (t_i) and the time (τ) between the nucleation and growth periods increase with increasing film thickness irrespective of anion species (borate and phosphate ions). In addition, they become much larger for the anodic films in the phosphate solution than for those in the borate solution.

(3) The pitting corrosion process during the pit nucleation period is independent of film thickness and anion species from the fact that the slope of the linear relationship between log i_p (pitting current density) and log t curve is the same irrespective of them.

(4) The slope of the linear relationship between log i_p (pitting current density) and log t curve during the pit growth period is larger for the anodic films in the borate than for that in the phosphate. The former and latter slopes are smaller and larger than that in the pit nucleation period.

(5) The results thus obtained are reasonably explained in terms of the ion-selectivity of the outer layer incorporated with anion species and the solution inside the pit; the anodic films in the borate solution show anion-selectivity and those in the phosphate solution have cation-selectivity as well as those of the solution inside the pit.

References

1. Foley RT (1986) Localized corrosion of aluminum-alloys - a review. Corros 42 (5):277-288

2. Szklarska-Smialowska Z (1999) Pitting corrosion of aluminum. Corros Sci 41

(9):1743-1767

3. Moutarlier V, Gigandet MP, Pagetti J (2003) Characterisation of pitting corrosion in sealed anodic films formed in sulphuric, sulphuric/molybdate and chromic media. Appl Surf Sci 206 (1-4):237-249

4. Trueman AR (2005) Determining the probability of stable pit initiation on aluminium alloys using potentiostatic electrochemical measurements. Corros Sci 47 (9):2240-2256

5. Yu SY, O'Grady WE, Ramaker DE, Natishan PM (2000) Chloride ingress into aluminum prior to pitting corrosion - an investigation by XANES and XPS. J Electrochem Soc 147 (8):2952-2958

6. Zaid B, Saidi D, Benzaid A, Hadji S (2008) Effects of ph and chloride concentration on pitting corrosion of AA6061 aluminum alloy. Corros Sci 50 (7):1841-1847

7. Lee W-J, Pyun S-I (2000) Effects of sulphate ion additives on the pitting corrosion of pure aluminium in 0.01 M NaCl solution. Electrochim Acta 45 (12):1901-1910

8. Na K-H, Pyun S-I (2006) Effect of sulphate and molybdate ions on pitting corrosion of aluminium by using electrochemical noise analysis. J Electroanal Chem 596 (1):7-12

9. Na K-H, Pyun S-I (2007) Effects of sulphate, nitrate and phosphate on pit initiation of pure aluminium in HCl-based solution. Corros Sci 49 (6):2663-2675

10. Yamashita M, Miyuki H, Nagano H, Misawa T (1997) Compositional gradient and

ion selectivity of Cr-substituted fine goethite as the final protective rust layer on weathering steel. Tetsu to Hagane-J Iron Steel Inst Jpn 83 (7):448-453

11. Noda K, Nishimura T, Masuda H, Kodama T (1999) Ion selective permeability of the rust layer on Fe-Co and Fe-Ni low alloy steel. J Jpn Inst Met 63 (9):1133-1136
12. Noda K, Nishimura T, Masuda H, Kodama T (2000) Ion selectivity of rust formed on low-alloy steels under a cyclic wet-and-dry condition. J Jpn Inst Met 64 (9):767-770
13. Itagaki M, Nozue R, Watanabe K, Katayama H, Noda K (2004) Electrochemical impedance of thin rust film of low-alloy steels. Corros Sci 46 (5):1301-1310
14. Konishi H, Yamashita M, Uchida H, Mizuki J (2005) Structure analysis of cation selective Cr-goethite as protective rust of weathering steel. Mater Trans 46 (2):337-341
15. Nishimura T (2007) Structure of the rust on aluminum bearing steel after the exposure test. J Jpn Inst Met 71 (10):908-915
16. Nishimura R, Araki M, Kudo K (1984) Breakdown of passive film on iron. Corros 40 (9):465-470
17. Nishimura R (1987) Pitting corrosion of nickel in borate and phosphate solutions. Corros 43 (8):486-492
18. Wood GC, Skeldon P, Thompson GE, Shimizu K (1996) A model for the incorporation of electrolyte species into anodic alumina. J Electrochem Soc

143:74-83

19. Takahashi H, Fujimoto K, Konno H, Nagayama M (1984) Distribution of anions and protons in oxide films formed anodically on aluminum in a phosphate solution. J Electrochem Soc 131:1856

20. Takahashi H, Kasahara K, Fujiwara K, Seo M (1994) The cathodic polarization of aluminum covered with anodic oxide-films in a neutral borate solution .1. The mechanism of rectification. Corros Sci 36 (4):677-688

21. Takahashi H, Fujimoto K, Nagayama M (1988) Effect of ph on the distribution of anions in anodic oxide-films formed on aluminum in phosphate solutions. J Electrochem Soc 135 (6):1349-1353

22. Pringle JPS (1980) The anodic oxidation of superimposed metallic layers: Theory. Electrochim Acta 25:1423-1437

23. Brown F, Mackintosh WD (1973) The use of rutherford backscattering to study the behavior of ion-implanted atoms during anodic oxidation of aluminum: Ar, Kr, Xe, K, Rb, Cs, Cl, Br, i. J Electrochem Soc 120:1096-1102

24. Shimizu K, Thompson GE, Wood GC (1981) Electron-beam-induced crystallization of anodic barrier films on aluminium. Thin Solid Films 77:313-318

25. Shimizu K, Thompson GE, Wood GC, Xu Y (1982) Direct observation of ion-implanted xenon marker layer in anodic barrier films on aluminium. Thin Solid Films 88:255-262

26. Shimizu K, Kobayashi K, Thompson GE, Wood GC (1991) A novel marker for the determination of transport numbers during anodic barrier oxide growth on aluminium. Phil Mag B 64:345-353

27. Nishimura R, Kudo K, Sato N (1976) The potential dependence of composition of anodic passive film on iron in neutral solution J Jpn Inst Met 40 (2):118-124

28. Sato N, Kudo K, Nishimura R (1976) Depth analysis of passive films on iron in neutral borate solution. J Electrochem Soc 123 (10):1419-1423

29. Nishimura R, Kudo K, Sato N (1981) Passive films on iron in phosphate and borate solutions. J Jpn Inst Met 45 (6):581-587

30. Hagyard T, Williams JR (1961) Potential of aluminium in aqueous chloride solutions .Part 1. Trans Faraday Soc 57 (12):2288-2294

Figure Captions

Fig. 1 Transmission electron micrographs of ultramicrotomed sections of aluminum anodized to 100 V at 1 mA cm^{-2} in (a) the borate and (b) phosphate electrolytes.

Fig. 2 GDOES depth profiles of the anodic films formed on aluminum to 100 V at 1 mA cm^{-2} in (a) the borate and (b) phosphate electrolytes.

Fig. 3 Change in the pitting current density with time for the aluminum specimens at -0.6 V vs Ag/AgCl in 0.5 mol dm^{-3} NaCl solution at 293 K. Before the measurements, the aluminum specimens were anodized to several potentials at 1 mA cm^{-2} in the borate electrolyte. The broken line denotes the result of aluminum without anodizing.

Fig. 4 Double logarithmic plot of the pitting current density vs time for the aluminum specimens at -0.6 V vs Ag/AgCl in 0.5 mol dm^{-3} NaCl solution at 293 K. Before the measurements, the aluminum specimens were anodized to several potentials at 1 mA cm^{-2} in the borate electrolyte.

Fig. 5 Change in the pitting current density with time for the aluminum specimens at -0.6 V vs Ag/AgCl in 0.5 mol dm^{-3} NaCl solution at 293 K. Before the measurements, the aluminum specimens were anodized to several potentials at 1 mA cm^{-2} in the phosphate electrolyte.

Fig. 6 Double logarithmic plot of the pitting current density vs time for the aluminum specimens at -0.6 V vs Ag/AgCl in 0.5 mol dm^{-3} NaCl solution at 293 K. Before the measurements, the aluminum specimens were anodized to several potentials at 1 mA cm^{-2} in the phosphate electrolyte.

Fig. 7 Change in the incubation time with film thickness for the aluminum specimens anodized to several potentials at 1 mA cm^{-2} in the borate and phosphate electrolytes.

Fig. 8 Change in τ with film thickness for the aluminum specimens anodized to several potentials at 1 mA cm^{-2} in the borate and phosphate electrolytes.

Fig. 9 Schematic illustration showing the ingress rate of chloride ions in the anodic films formed in (a) borate electrolyte and (b) phosphate electrolyte.

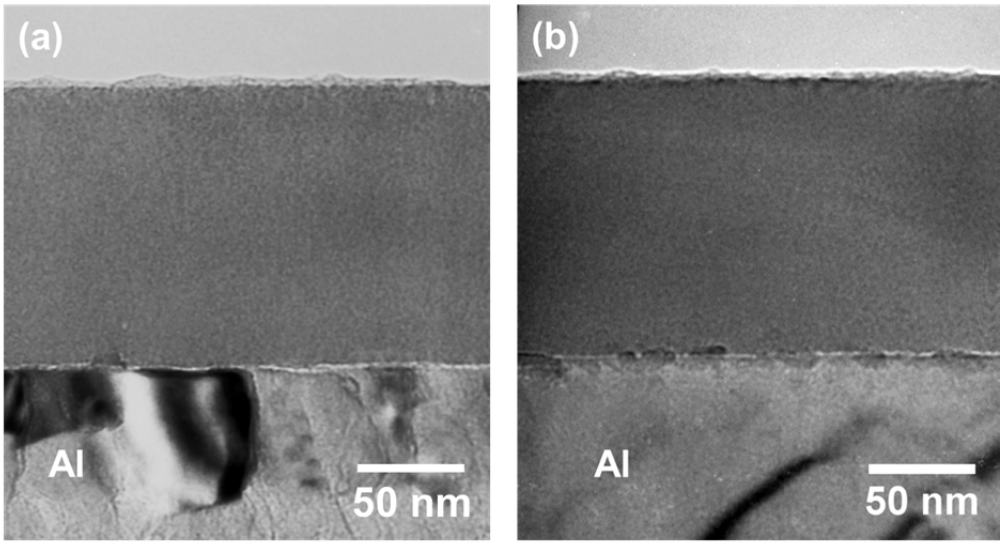

Fig. 1 Transmission electron micrographs of ultramicrotomed sections of aluminum anodized to 100 V at 1 mA cm^{-2} in (a) the borate and (b) phosphate electrolytes.

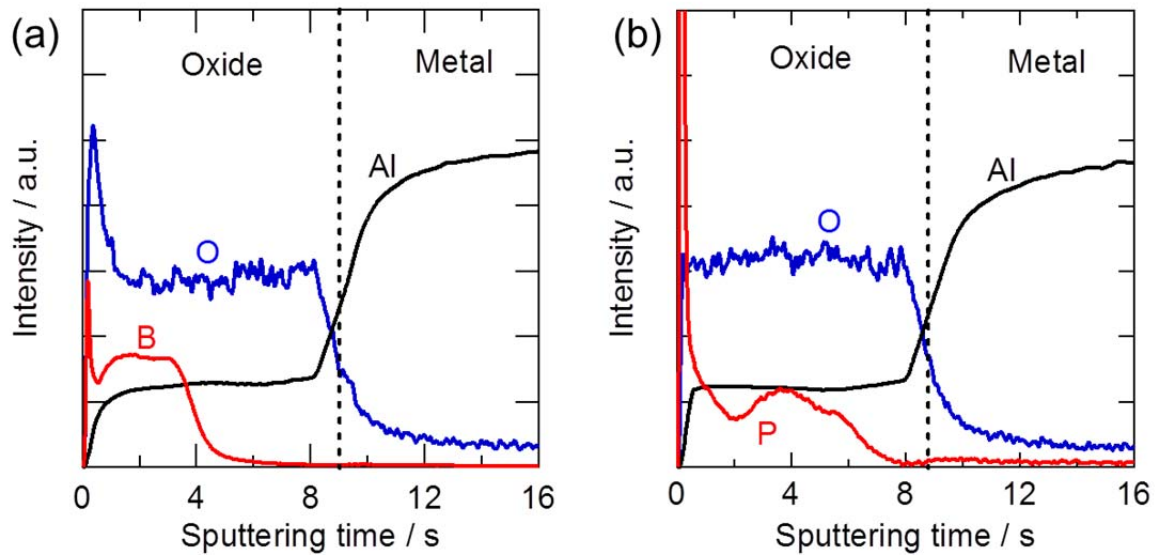

Fig. 2 GDOES depth profiles of the anodic films formed on aluminum to 100 V at 1 mA cm^{-2} in (a) the borate and (b) phosphate electrolytes.

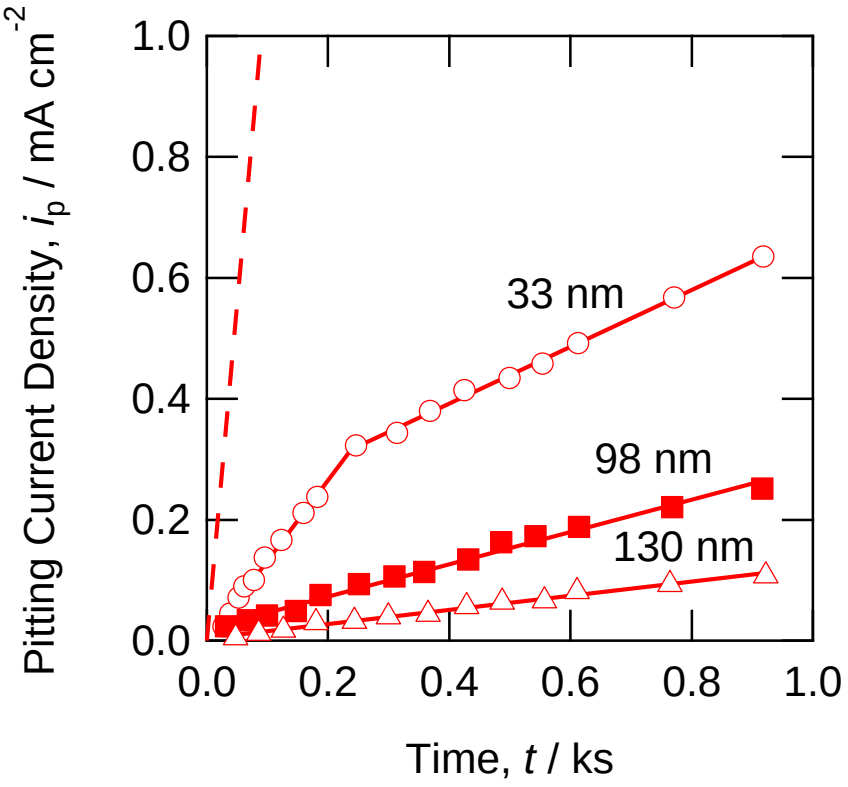

Fig. 3 Change in the pitting current density with time for the aluminum specimens at -0.6 V vs Ag/AgCl in 0.5 mol dm^{-3} NaCl solution at 293 K. Before the measurements, the aluminum specimens were anodized to several potentials at 1 mA cm^{-2} in the borate electrolyte. The broken line denotes the result of aluminum without anodizing.

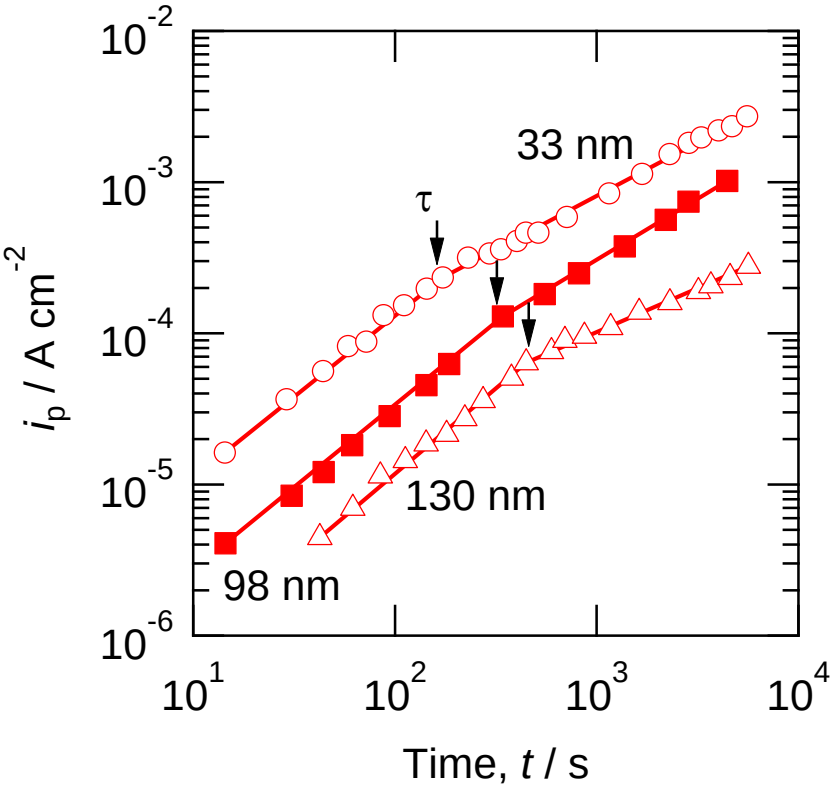

Fig. 4 Double logarithmic plot of the pitting current density vs time for the aluminum specimens at -0.6 V vs Ag/AgCl in 0.5 mol dm^{-3} NaCl solution at 293 K. Before the measurements, the aluminum specimens were anodized to several potentials at 1 mA cm^{-2} in the borate electrolyte.

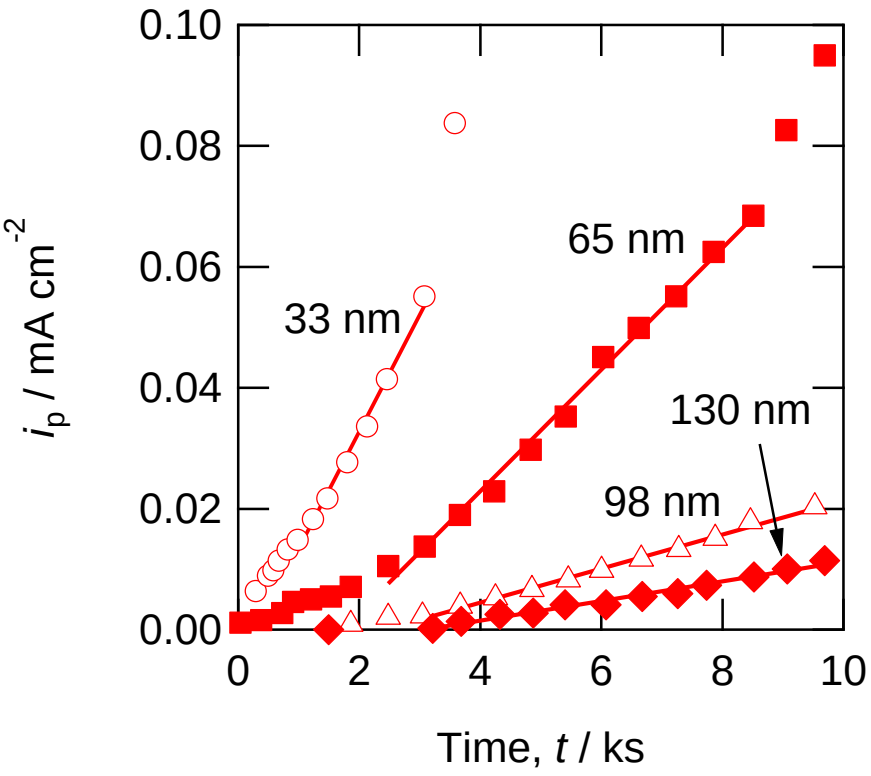

Fig. 5 Change in the pitting current density with time for the aluminum specimens at -0.6 V vs Ag/AgCl in 0.5 mol dm^{-3} NaCl solution at 293 K. Before the measurements, the aluminum specimens were anodized to several potentials at 1 mA cm^{-2} in the phosphate electrolyte.

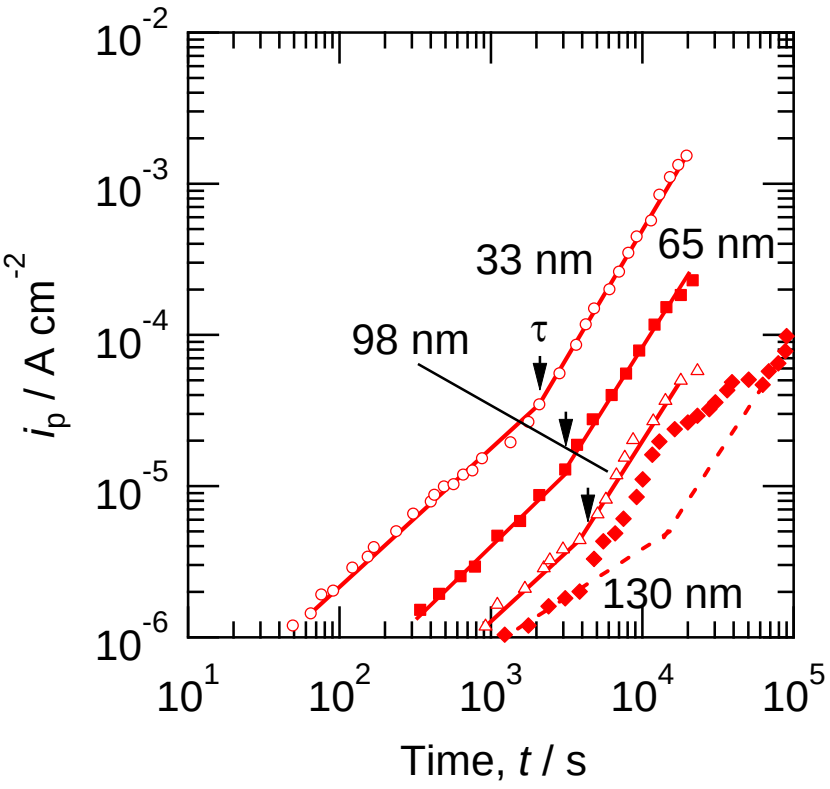

Fig. 6 Double logarithmic plot of the pitting current density vs time for the aluminum specimens at -0.6 V vs Ag/AgCl in 0.5 mol dm^{-3} NaCl solution at 293 K. Before the measurements, the aluminum specimens were anodized to several potentials at 1 mA cm^{-2} in the phosphate electrolyte.

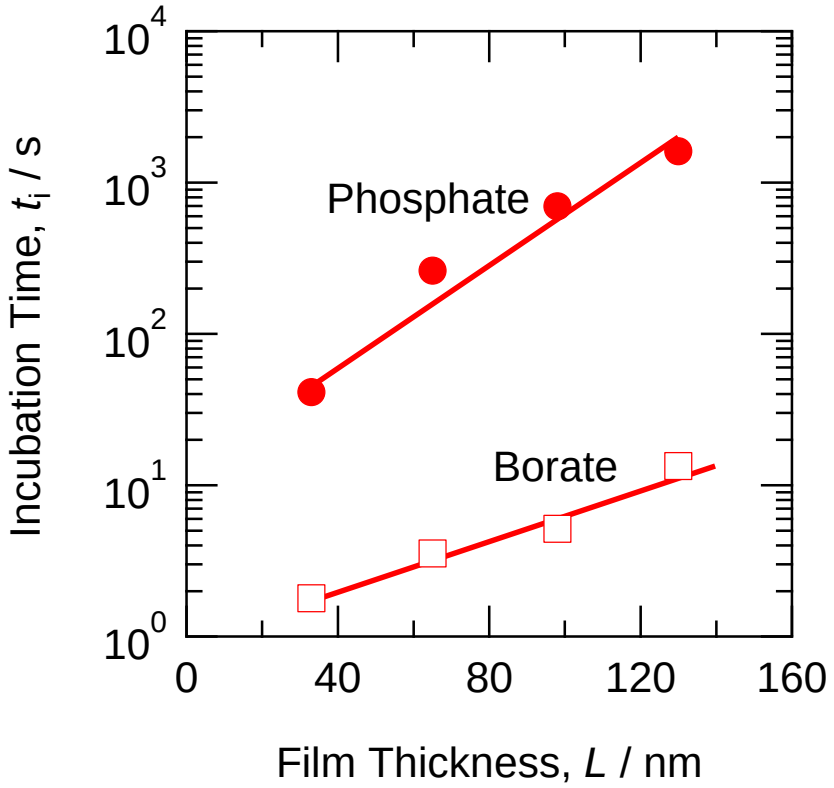

Fig. 7 Change in the incubation time with film thickness for the aluminum specimens anodized to several potentials at 1 mA cm^{-2} in the borate and phosphate electrolytes.

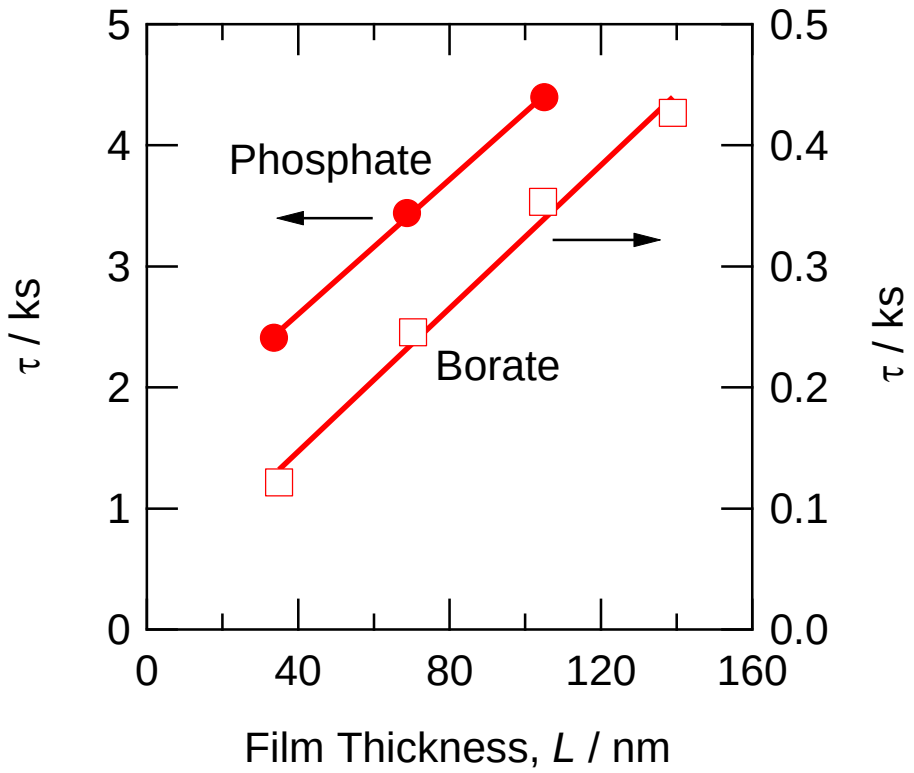

Fig. 8 Change in τ with film thickness for the aluminum specimens anodized to several potentials at 1 mA cm^{-2} in the borate and phosphate electrolytes.

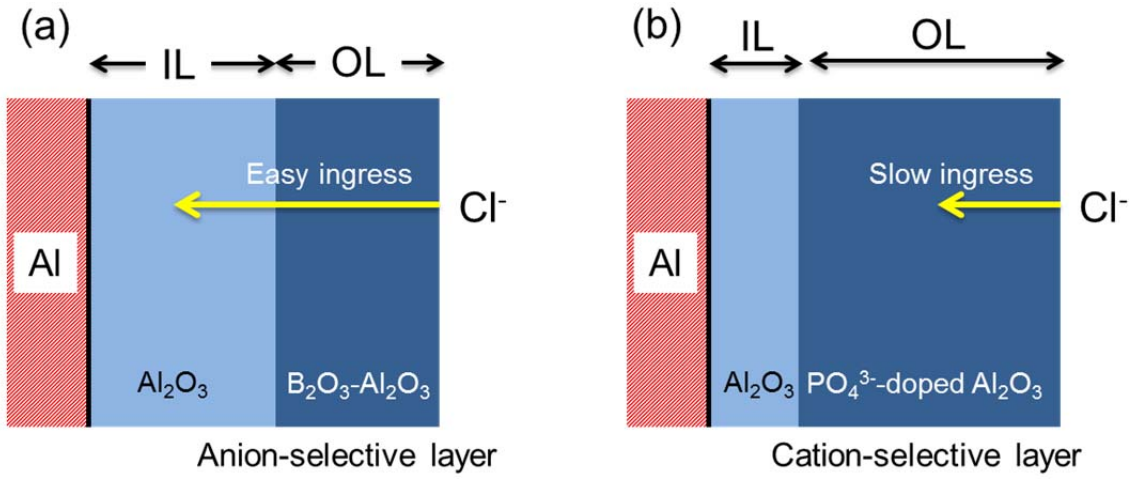

Fig. 9 Schematic illustration showing the ingress rate of chloride ions in the anodic films formed in (a) borate electrolyte and (b) phosphate electrolyte.